J Mater Sci (2011) 46:7588–7593
DOI 10.1007/s10853-011-5734-y

Influence of sputtering pressure on the structure and ionic conductivity of thin film amorphous electrolyte

Zongqian Hu · Kai Xie · Di Wei · Najeeb Ullah

Received: 28 January 2011 / Accepted: 21 June 2011 / Published online: 29 June 2011

Abstract Ionic conducting thin film amorphous electrolytes are promising candidates for microelectronics applications. This study presents an investigation into the structure and composition of lithium phosphorus oxynitride (LiPON) thin film electrolyte prepared using radio frequency (RF) sputtering on Li_3PO_4 target. The ionic conductivity of LiPON thin films has been dramatically improved by decreasing N_2 pressure. X-ray photoelectron spectra (XPS) were used to determine the structure and composition of LiPON thin films. It was found that increasing the N_2 pressure during the deposition process resulted in a greatly decreased formation of triply coordinated –N<(N_t) as compared to doubly coordinated –N=(N_d) in LiPON thin films. These results indicate that the N_t structural unit plays an important role in the improvement of ionic conductivity as compared to the N_d structural unit. It also shows that PO_2N_2 tetrahedra with two N_t structural units exist in LiPON thin films at low N_2 pressures. Consequently, the improved ionic conductivity of the LiPON thin film deposited at low pressure results from the existence of PO_2N_2 tetrahedra with two N_t structural units in LiPON thin film. PO_2N_2 tetrahedra with two N_t structural units provides higher cross-linking density of the glass network and lower electrostatic energy than with two N_d structural units.

Z. Hu (✉) · K. Xie
School of Aerospace and Materials Engineering, National University of Defense Technology, Changsha 410073, Hunan, People's Republic of China
e-mail: huzongqian@gmail.com

Z. Hu · N. Ullah
Department of Materials Science and Metallurgy, University of Cambridge, Cambridge CB2 3QZ, UK

D. Wei
Nokia Research Centre, 21 JJ Thompson Avenue, Cambridge CB3 0FA, UK

Introduction

Thin film amorphous lithium-ion conductive electrolytes have been applied in various devices such as microbatteries, sensors, and electrochromic windows [1, 2]. Of these electrolytes, lithium phosphorous oxynitride (LiPON) thin film electrolyte, with high lithium-ion conductivity and good stability in contact with lithium metal is an attractive candidate for microelectronics including microbatteries [3, 4] and microsupercapacitors [5, 6]. Moreover, these thin films can be used as protective layers in lithium batteries and electrochromic devices [7, 8].

Since realizing that these thin films were promising solid electrolytes [9–11], researchers have reported on various composition and conductivity of LiPON thin films deposited using radio frequency (RF) magnetron sputtering [12, 13]. However, only a few studies are known on the influence of the structure on the ionic conductivity [14, 15]. The observed increase in ionic conductivity is supposed to be related to the formation of P–N bonds which replace P–O bonds making it a more reticulated anionic network [14]. Different structural investigations evidence the existence of two nitrogen species in LiPON thin films. These are triply coordinated –N<(N_t) and doubly coordinated –N=(N_d) [14, 16, 17]. However, the distribution of these two nitrogen species has not been thoroughly investigated. Iriyama et al. [18] have reported that thermal annealing changed the peak intensities of the N_t and N_d. This finding sensibly implies that the properties of LiPON thin films depend upon the preparation conditions and that maximum ionic conductivity of the resulting thin films can be

optimized by careful adjustments of these conditions. This realization makes understanding thin film structural property correlations, and how preparation conditions can influence thin film composition, important.

In this article, three series of LiPON thin films have been prepared using RF magnification sputtering under various N_2 pressures. The main objective is correlating the ionic conductivity with thin films structure by investigating the effect of structural changes on the ionic conductivity of LiPON thin films. The effect of N_2 pressure on the structural change of LiPON thin films was also investigated.

Experimental

Sample preparation

LiPON thin films were deposited using RF magnetron sputtering from a Li_3PO_4 target in an ambient nitrogen atmosphere. To obtain the sputtering target, Li_3PO_4 powder (Aldrich, 99.9%) was pressed under a 100 kg cm^{-2} load and sintered it at 850 °C for 6 h. The sintered pellet was finally worked into a target of 60 mm in diameter. Silicon (100) substrates with both surfaces optically polished were cleaned in acetone, methanol, and ethanol for 5 min and rinsed thoroughly with deionized water. In order to evaluate electrolyte properties such as ion conductivity and activation energy, the blocking electrode structure for lithium ions was stacked in the form of Au/LiPON/Au on the substrate. Au thin films (300 nm) were deposited on the wafer. LiPON thin films were deposited on Au thin films in nitrogen atmosphere (99.999%) using RF reactive sputtering. During sputtering, the substrate temperature was controlled between 10 and 15 °C, and working pressures were 10, 40, and 60 mTorr, for the three series. Finally, upper Au thin films were deposited on the LiPON thin films using direct current (DC) magnetron sputtering. Deposition time was controlled in order to obtain films with thicknesses in the range ~1 μm. The detailed deposition conditions of LiPON thin films are presented in Table 1.

Table 1 Deposition conditions for LiPON thin film solid electrolyte

Variables	Conditions
Target	Sintered Li_3PO_4 (60 mm dia.)
Substrate	Silicon wafer (100)
Base pressure	6.0×10^{-6} Torr
Working gas	99.999% N_2
Process working pressure	10, 40, 60 mTorr
Sputtering power	RF 120 W
Substrate temperature	10–15 °C
Thickness	~1 μm
Distance between target and substrate	60 mm

Characterization of the sample

The micro-structure of LiPON thin films was analyzed by X-ray diffraction (XRD, Rigaku, D/max 2500). The nitrogen/phosphorus ratio of LiPON thin films was determined by energy dispersive spectroscopy (EDS, Hitachi, S-4800). The ionic conductivity of LiPON thin films was obtained from an electrochemical impedance spectroscopy (EIS, AUTOLAB, PGSTAT100) of the Au/LiPON/Au sandwich structure fabricated on silicon wafer. The alternating current (AC) response of the samples ranging from 1 Hz to 1 MHz at various temperatures was measured by an AUTOLAB frequency response analyzer and an AUTOLAB electrochemical interface. The ionic conductivity (σ) of LiPON thin films was obtained using $\sigma = d/(R \times A)$ [19], where d is the film thickness determined by scanning electron microscopy (SEM, Jeol, JSM-6360LV), A is the electrode area and R is the film resistance determined by the low frequency intersection of the semicircle with the x-axis in the Nyquist diagrams. The impedance calculating the ionic conductivity was measured at 25 °C, and the activation energy (E_a) was measured at a 15 °C increment from 25 to 85 °C.

X-ray photoelectron spectra (XPS) measurements were performed using an electron spectroscopy system (Kratos, Xsam 800) equipped with an Mg Kα (1253.6 eV) monochromatic source. In order to obtain accurate results, an Ar^+ ion sputtering was carried out on the LiPON thin films samples prior to XPS measurements. Survey scans were made from 1000 to 0 eV, and high resolution spectra were taken in the Li_{1s}, N_{1s}, O_{1s}, P_{2p}, and C_{1s} regions. These core level spectra were referenced to the C_{1s} line at 285.0 eV. Asymmetric N_{1s} and O_{1s} peaks were resolved using a curve fitting assuming two or three components in the respective regions. Data analysis and the curve fitting were resolved by the XPSPEAK41 procedure. In XPSPEAK41, the experimental data were analyzed by a method of non-linear least-squares curve fitting. Each data set was first corrected for the non-linear emission background using a Shirley function and then fitted with mixed Gaussian–Lorentzian functions [20, 21].

Results and discussion

The XRD patterns of the Li_3PO_4 target and LiPON thin film deposited at various N_2 pressures are shown in Fig. 1. The Li_3PO_4 target exhibits a typical well-crystallized phase but only the diffraction peak of silicon wafer substrate is recorded in each LiPON thin film. This indicates that

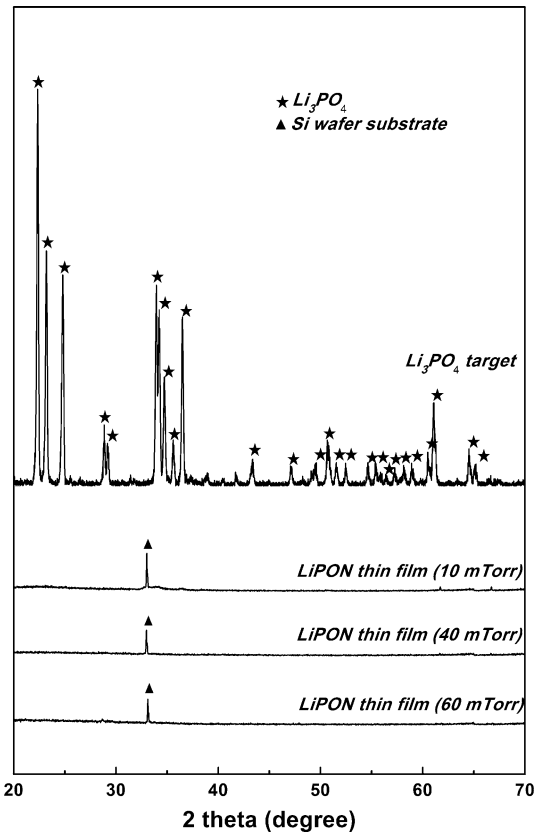

Fig. 1 XRD patterns of Li_3PO_4 target and LiPON thin films with various N_2 pressures

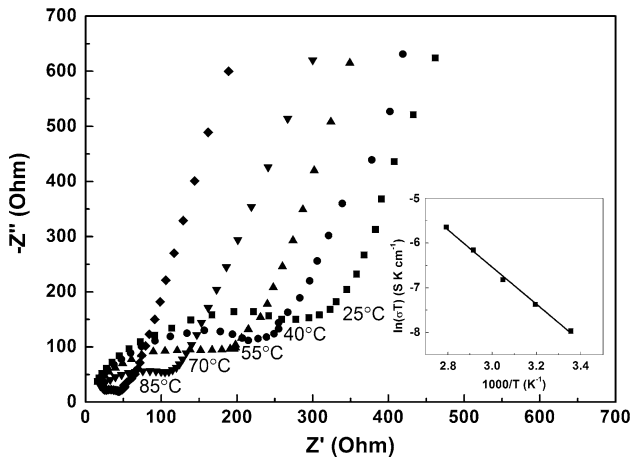

Fig. 2 Nyquist diagrams of the LiPON thin films deposited at 10 mTorr for various temperatures. Illustration is Arrhenius plots for conductivity of the LiPON thin film deposited at 10 mTorr

LiPON thin films are amorphous and independent of N_2 pressure.

Complex impedance analysis of the electrical data was carried out to determine the electrical conductivity of LiPON thin films deposited at various N_2 pressures. Figure 2 shows the Nyquist diagrams of the LiPON thin films deposited at 10 mTorr at 25, 40, 55, 70, and 85 °C. The illustration presents the logarithm of ionic conductivity as a function of the reciprocal absolute temperature for LiPON thin film deposited at 10 mTorr. The plot of $\ln(\sigma)$ against $1000/T$ is found to be linear and well-fitted by the Arrhenius equation, $\sigma T = \sigma_o \exp(-E_a/\kappa T)$ [16].

The ionic conductivity at 25 °C and the activation energy for various deposited pressures are shown in Fig. 3. It shows a decrease in lithium ion conductivity and an increase in activation energy of LiPON thin films as N_2 pressures increase from 10 to 60 mTorr. These results agree with a previous study by Park et al. [22]. Maximum conductivity of $1.5 \pm 0.1 \times 10^{-6}$ S cm^{-1} was obtained for a LiPON thin film deposited at 10 mTorr with $E_a = 0.37 \pm 0.01$ eV. This conductivity is one to two orders of magnitude higher than those of the thin films deposited at 40 and 60 mTorr. The composition and the structural changes brought about by the nitrogen atom incorporation into the glass network could be a reason for the decrease of in the conductivity with increasing N_2 pressure. The reason for the decrease of the lithium ion conductivity in the LiPON thin films deposited under high N_2 pressure and the effect of nitrogen incorporation into the glass network still remains controversial [15, 23, 24].

LiPON amorphous thin films composition are shown in Table 2. As N_2 pressure increases, the lithium and oxygen contents increases while the nitrogen content decreases.

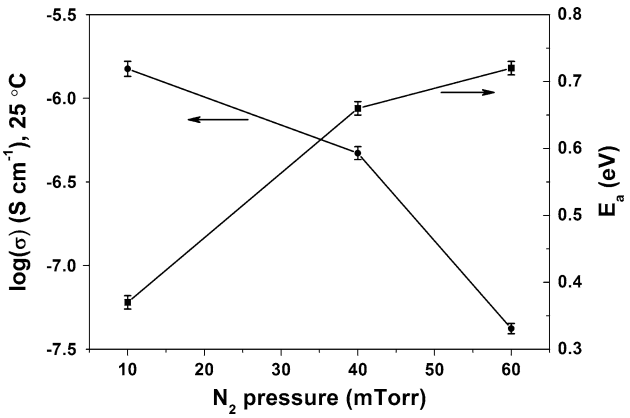

Fig. 3 Ionic conductivity and activation energy of LiPON thin films deposited at 10, 40, and 60 mTorr

Table 2 Composition (atoms) of LiPON thin films deposited at various N_2 pressure measured by XPS

Nitrogen pressure (mTorr)	Li	P	O	N
10	2.02	1.0	3.05	0.74
40	3.04	1.0	4.19	0.58
60	4.13	1.0	5.21	0.36

Owing to the shorten mean-free-path and larger probability of the scattering sputtered particles, it is assumed that the kinetic energy of the sputtered particles colliding with the substrate is high and thus the re-sputtering probability of lithium, being a light element, increases. Therefore, the high re-sputtering probability of lithium results in the less lithium content at low N_2 pressure. The oxygen and nitrogen contents are thought to be related to the substitution of nitrogen for oxygen. More oxygen content and less nitrogen content are observed at the high pressure (40, 60 mTorr) deposited films. This is due to the low kinetic energy of the sputtered particles at high pressures, which makes the substitution of nitrogen for oxygen more difficult. On the other hand, nitrogen ions (N^+, N^{2+}) density in the plasma decrease when other process parameters, such as sputtering power, are held constant. The probability of collisions between sputtered particles and nitrogen ions is believed to be lower during LiPON thin films formation. The nitrogen level of LiPON thin film decreases as N_2 pressures increase from 10 to 60 mTorr.

The XPS core level O_{1s} spectra of LiPON thin films deposited at 10, 40, and 60 mTorr are shown in Fig. 4. The O_{1s} spectra can be divided into three components which correspond to two types of non-bridging oxygen (P=O (O_d), Li^+…O–P (O_{nb})) and one bridging oxygen (P–O–P (O_b)) [16, 25]. The ratios of different environment of oxygen at various N_2 pressures determined from their respective areas from the XPS spectra are listed in Table 3. The O_{nb} content remains the same and is independent of N_2 pressure. This result agrees with Sauze et al. [26]. As N_2 pressure increase, O_b content increases sharply while O_d content decreases. This result indicates that less nitrogen is replaced the O_b structural unit in PO_4 tetrahedra while more nitrogen replaced the O_d structural unit at high pressure in the three series of pressures tested.

The effect of N_2 pressure on the XPS core level N_{1s} spectra of LiPON thin films is shown in Fig. 5. Asymmetric N_{1s} spectra of LiPON thin films were observed around 398 eV and can be resolved into two peaks. These peaks are assigned to the nitrogen bonds of doubly

Table 3 Observed and calculated ratios of nitrogen and oxygen in LiPON thin films deposited at various N_2 pressure

N_2 pressure (mTorr)	$\frac{O_b}{O_b+O_d+O_{nb}}$	$\frac{O_d}{O_b+O_d+O_{nb}}$	$\frac{O_{nb}}{O_b+O_d+O_{nb}}$
10	0.04	0.60	0.36
40	0.07	0.59	0.36
60	0.12	0.51	0.37

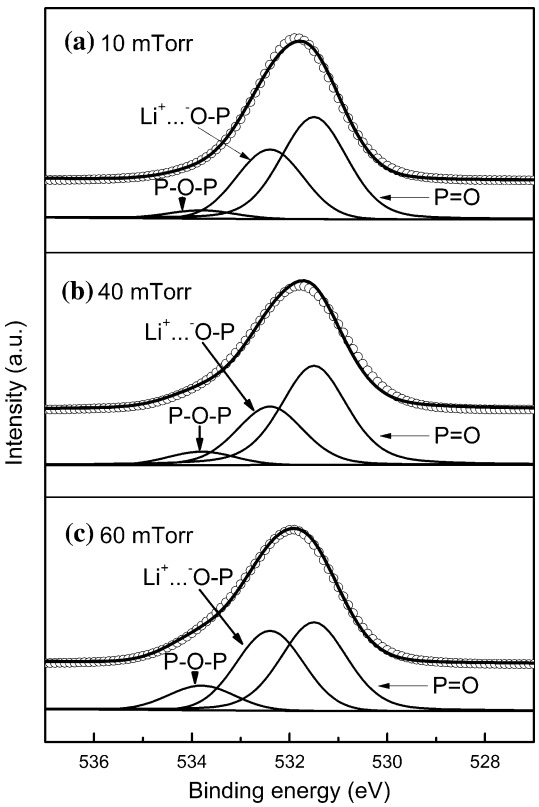

Fig. 4 O_{1s} XPS spectra of LiPON thin films deposited at different N_2 pressures

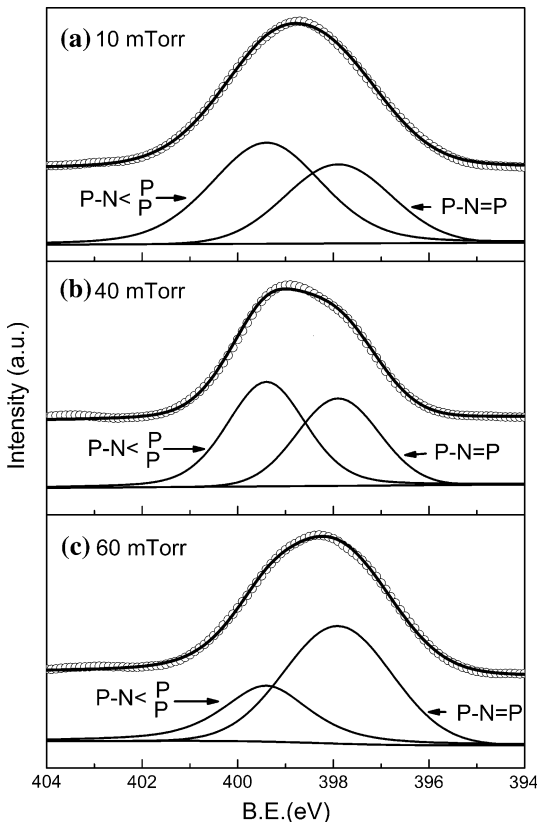

Fig. 5 N_{1s} XPS spectra of LiPON thin films with various N_2 pressure

Table 4 Observed and calculated ratios of nitrogen in LiPON thin films with various N_2 pressure

N_2 pressure (mTorr)	N/P EDS (±0.01)	N/P XPS	N_t/P	N_d/P	N_t/N_d
10	0.70	0.74	0.45	0.29	1.54
40	0.57	0.58	0.32	0.25	1.29
60	0.34	0.36	0.12	0.24	0.50

coordinated –N=(N_d) at 397.9 eV and triply coordinated –N<(N_t) at 399.4 eV [17]. The quantitative measure of each bond is calculated from the area of the curve corresponding to the assigned bond in the photoelectron spectra for LiPON thin films and is listed in Table 4. The N/P ratios determined by XPS largely agree with those obtained by energy dispersive spectroscopy (EDS). Increasing the N_2 pressure sharply decreases in the N_t/P and N_t/N_d ratio. This is not so for the N_d/P ratio. These results indicate that N_t structural unit formation is more difficult than N_d structural unit formation at high N_2 pressure. By comparing the variations in the molecular structures of LiPON thin films deposited at various N_2 pressures with their ionic conductivities shown in Table 2, it appears that the N_t structural unit plays an important role in the increased ionic conductivity if compared to N_d structural unit.

It is reported that nitride phosphate glasses are composed of PO_4, PO_3N, and PO_2N_2 tetrahedra [27]. If nitride phosphate glasses are only composed of PO_3N tetrahedra, these glasses should have an N_t/P ratio equal to 1/3 and an N_d/P ratio equal to 1/2 [16]. As shown in Table 4, the maximum ratios of N_t/P and N_d/P for LiPON thin films deposited at 40 and 60 mTorr remains lower than 1/3 and 1/2, respectively. Therefore, the presence of two N_t and N_d structural units in the same tetrahedron is excluded. The reaction scheme of phosphate chain with nitrogen in the LiPON thin film deposited at high pressure (40, 60 mTorr) is shown in Scheme 1a–c. The N_t/P ratio of LiPON thin film deposited at low pressure (10 mTorr) is 0.45. Nitrogen/oxygen substitution of PO_2N_2 tetrahedra with two N_t structure units shown in Scheme 1d exists in LiPON thin films.

According to the model by Marchand et al. [17], N_t structural unit is linked to three phosphorus atoms, whereas N_d structural unit is only bridged between two phosphorus atoms. N_t structural unit provides a higher cross-linking density of the glass network of LiPON thin films. It appears that introducing two N_t structure units results in breaking three P–O–P bonds, while there is only one P–O–P bond break in two N_d structure units. This contributes to a decrease in electrostatic energy from the N_t structural unit

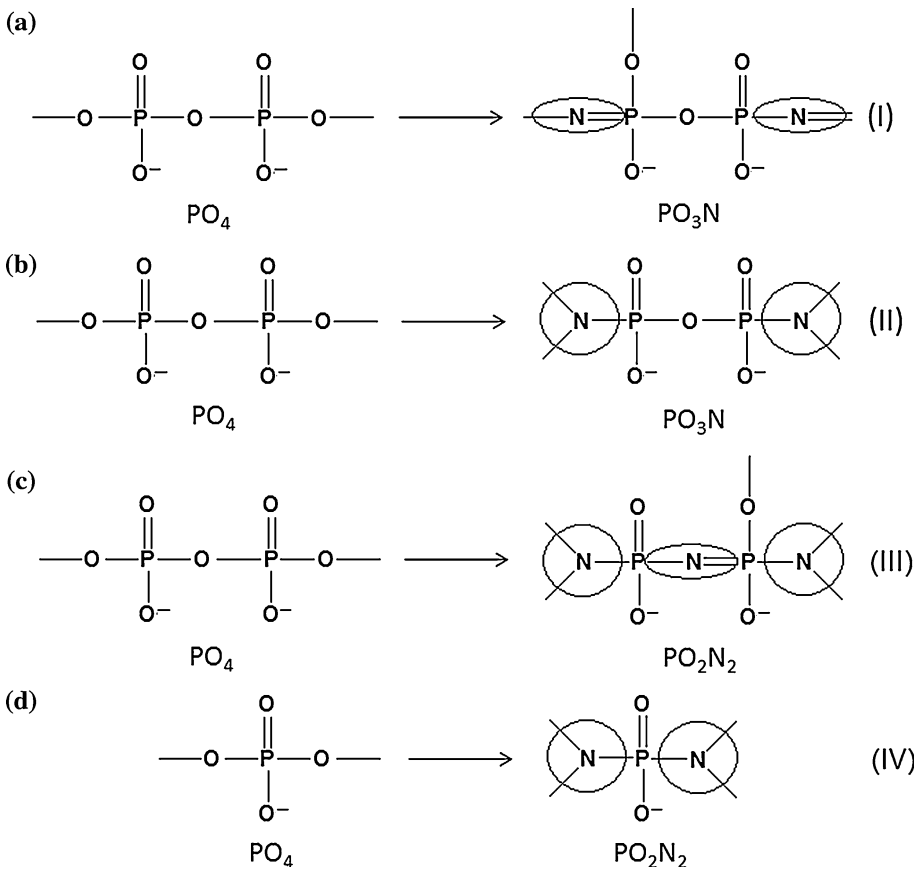

Scheme 1 Reaction scheme of phosphate chain with nitrogen for LiPON thin film deposited at various pressures

by substituting P–O bond with P–N bond (which is more covalent) and far more than that from N_d structural unit. PO_2N_2 tetrahedra, by having two N_t structure units (type-IV), provides higher cross-linking density of the glass network and lower electrostatic energy than other nitride phosphate tetrahedra (type I–III). Consequently, increasing N_t content in LiPON thin films with a high glass density and a low O_b content at low N_2 pressure should increase the conductivity of LiPON thin film.

Conclusions

The influence of the molecular structure changes on the ionic conductivity of LiPON thin films which were deposited at various N_2 pressures has been studied. It was observed that ionic conductivity of LiPON thin films increases when N_2 pressure decreases with the maximum ionic conductivity of $1.5 \pm 0.1 \times 10^{-6}$ S cm^{-1} obtained at 10 mTorr. The changes in structure and composition (N_t, N_d) of LiPON thin films were thoroughly investigated at various N_2 pressures by a XPS structural study. The sharp decrease in N_t content at high N_2 pressure confirms that N_t structural unit plays an important role in the improving ionic conductivity of LiPON thin films. It also found that PO_2N_2 tetrahedras with two N_t structural units exist in LiPON thin films at low N_2 pressure. This structure has more N_t structural units than other PO_3N and PO_2N_2 tetrahedra (type I–III). We conclude that the LiPON thin films deposited at low pressure have high ionic conductivity which is due to the presence of PO_2N_2 tetrahedra with two N_t structural units in LiPON thin film by providing higher cross-linking density in the glass network and lower electrostatic energy than other nitride phosphate tetrahedras.

References

1. Vinatier P, Hamon Y (2006) In: Baranovski S (ed) Charge transport in disordered solids with applications in electronics. John Wiley and Sons, New York
2. Jee SH, Oh JY, Ahn HS, Kim D-J, Wikle HC III, Kim SH, Yoon YS (2010) J Mater Sci 45:1709. doi:10.1007/s10853-009-3904-y
3. Bai Y, Knittlmayer C, Gledhill S, Lauermann I, Fischer C-H, Weppner W (2009) Ionics 15:11
4. Lu H-W, Yu L, Zeng W, Li Y-S, Fu Z-W (2008) Electrochem Solid State Lett 8:A140
5. Lee M-J, Kim JS, Choi SH, Lee JJ, Kim SH, Jee SH, Yoon YS (2006) J Electroceram 17(2–4):639
6. Yoon YS, Cho WI, Lim JH, Choi DJ (2001) J Power Sources 101:126
7. Yoo SJ, Lim JW, Choi B, Sung Y-E (2007) J Electrochem Soc 154:6
8. Yoo SJ, Lim JW, Sung Y-E (2006) Sol Energy Mater Sol Cells 90:477
9. Rho N-S, Lee S-D, Kwon H-S (1999) Scripta Mater 42:43
10. Bates JB, Dudney NJ, Gruzalski GR, Zuhr RA, Choudhury A, Luck CF, Robertson JD (1993) J Power Sources 1–3:103
11. Yu X, Bates JB, Jellison GE Jr, Hart FX (1997) J Electrochem Soc 2:524
12. Choi CH, Cho WI, Cho BW, Kim HS, Yoon YS, Tak YS (2002) Electrochem Solid State Lett 1:A14
13. Bates JB, Gruzalski GR, Dudney NJ, Luck CF, Yu X (1994) Solid State Ionics 70–71:619
14. Muñoz F, Durán A, Pascual L, Montagne L, Revel B, Rodrigues ACM (2008) Solid State Ionics 179:574
15. Wang B, Kwak BS, Sakes BC, Bates JB (1995) J Non Cryst Solids 183:297
16. Li C-L, Fu Z-W (2007) J Electrochem Soc 154:A784
17. Le Sauze A, Montagne L, Palavit G, Marchand R (2001) J Non Cryst Solids 293–295:81
18. Iriyama Y, Kako T, Yada C, Abe T, Ogumi Z (2005) Solid State Ionics 176:2371
19. Yu XH, Bates JB, Jellison GE, Har l FX (1997) J Electrochem Soc 144:524
20. Aswal DK, Muthe KP, Tawde S, Chodhury S, Bagkar N, Singh A, Gupta SK, Yakhmi JV (2002) J Cryst Growth 236:661
21. Rochefort D, Dabo P, Guay D, Sherwood PMA (2003) Electrochim Acta 48:4245
22. Park HY, Nam SC, Lim YC, Choi KG, Lee KC, Park GB, Lee SR, Kim HP, Cho SB (2006) J Electroceram 17:1023
23. Unuma H, Sakka S (1987) J Mater Sci Lett 6:996
24. Unuma H, Komori K, Sakka S (1987) J Non Cryst Solids 95&96:913
25. Brückner R, Chun H-U, Goretzki H, Sammet M (1980) J Non Cryst Solids 42:49
26. Le Sauze A, Montagne L, Palavit G, Fayon F, Marchand R (2000) J Non Cryst Solids 263&264:139
27. Reidmeyer MR, Day DE (1995) J Non Cryst Solids 8:201